

Effect of Aqueous Environment on High Cycle and Very-High-Cycle Fatigue Behavior for a Structural Steel

HONG Youshi^{1, a} and QIAN Gui'an^{2, b}

¹LNM, Institute of Mechanics, Chinese Academy of Sciences, Beijing 100190, China

²PSI - Paul Scherrer Institute, Laboratory for Nuclear Materials, CH-5232 Villigen, Switzerland

^ahongys@imech.ac.cn, ^bGuian.Qian@psi.ch

Keywords: Very-high-cycle fatigue, aqueous environment, fatigue strength, fatigue crack initiation, fatigue crack propagation, structural steel.

Abstract. In this paper, rotary bending fatigue tests for a structural steel were performed in laboratory air, fresh water and 3.5% NaCl aqueous solution, respectively, thus to investigate the influence of environmental media on the fatigue propensity of the steel, especially in high cycle and very-high-cycle fatigue regimes. The results show that the fatigue strength of the steel in water is remarkably degraded compared with the case tested in air, and that the fatigue strength in 3.5% NaCl solution is even lower than that tested in water. The fracture surfaces were examined to reveal fatigue crack initiation and propagation characteristics in air and aqueous environments.

Introduction

Very-high-cycle fatigue (VHCF) [1] of metallic materials is regarded as fatigue failure at stress levels below conventional fatigue limit and the relevant fatigue life beyond 10^7 loading cycles. The research of VHCF has become a new horizon in metal fatigue since the early work contributed by Naito *et al.* [2]. In recent years, the investigation on VHCF of metallic materials has attracted an increasing number of investigators in fatigue research field, e.g. [3-5], due to the growing requirements of engineering applications, including aircraft, automobile, ship, railway, bridge, etc, for which the metallic components and structures need to endure the fatigue life larger than 10^7 loading cycles. The investigations on VHCF behavior of high strength steels available in literature were almost associated with the environment of laboratory air, and there were only a few investigations regarding the effect of environmental medium on VHCF behavior of high strength steels, e.g. [6]. The investigation on the fatigue strength difference caused by environmental effect (corrosion fatigue) in VHCF regime is of scientific interests and engineering importance.

In this paper, a structural steel (0.4%C, 1%Cr) was tested with a rotary bending machine operating at a frequency of 52.5Hz and the testing environments were of three types: laboratory air, fresh water and 3.5% NaCl aqueous solution, respectively, so as to investigate the influence of environmental medium on the variation of fatigue strength and cracking process. In addition, hour-glass type specimens with V-notch were used to investigate the process of fatigue crack propagation by taking the advantage of low temperature fracture technique. Based on the fatigue testing data and the scanning electron microscopy (SEM) observations of fracture surfaces, the effects of environment on the fatigue behavior at high cycle and VHCF regimes were examined. The mechanism of crack initiation and propagation under different environmental media was discussed.

Material and Experimental Method

The material tested in this investigation was a structural steel with main chemical compositions (wt %) of: 0.4C, 1Cr, 0.65Mn, 0.3Si and balance Fe. Hour-glass shape specimens were machined with the minimum diameter of 3mm and the round notch radius of 7mm. The raw specimens were heated at 1118K for 2 hours and oil quenched, then tempered at 473K for 1 hour and air-cooled. Such heat-treated specimens were of tempered martensite microstructure. The average size of original

austenite grains was 11.2 μm measured from 200 grains of intergranular morphology on SEM micrographs taken of fracture surfaces. The average ultimate tensile strength was 1582MPa from the tensile tests on 4 cylindrical specimens (5mm in diameter and 30mm in gage length).

Fatigue tests were performed by using a cantilever-type rotary bending machine at room temperature, which was operated at the frequency of 52.5 Hz. A weight piece was placed to the end of specimen through a fixture, which was converted to the applied maximum stress by a simple relation. Due to the feature of rotary bending scheme, the stress ratio was -1 throughout the tests. Three types of environmental media were used in the fatigue testing, namely laboratory air, fresh water and 3.5% NaCl aqueous solution. The experimental solution was controlled to drip onto the specimen surface (10-15 drops per minute) through a plastic tube from a reserved tank, such that enabled the specimen surface to maintain wet condition.

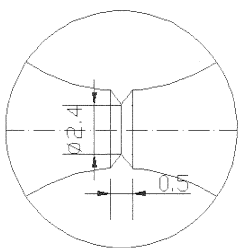


Fig. 1 V-notch profile at reduced section of hour-glass specimen (dimensions in mm).

For further examination of fatigue crack propagation in 3.5% NaCl solution, a group of hour-glass type specimens with V-notch at reduced section (Fig. 1) were cyclically loaded at the given maximum stress that corresponded to the fatigue strength at VHCF regime. One specimen was loaded to fatigue failure, and the others were controlled to terminate at different loading cycles before failure. Such terminated specimens were broken by means of low temperature fracture technique, i.e. each terminated specimen was broken immediately after immersed in liquid nitrogen for 20 minutes, such that the morphology produced during fatigue crack propagation was separated by the morphology formed at low temperature.

Results and Discussion

Fatigue Strength. The results of fatigue strength representing by S-N curves for specimens tested in laboratory air, water and 3.5% NaCl solution are shown in Fig. 2. For fatigue testing in laboratory air, as shown in the upper part of Fig. 2, the S-N curve exhibits a stepwise shape, for which the fatigue failure occurs at stress levels below the conventional fatigue limit.

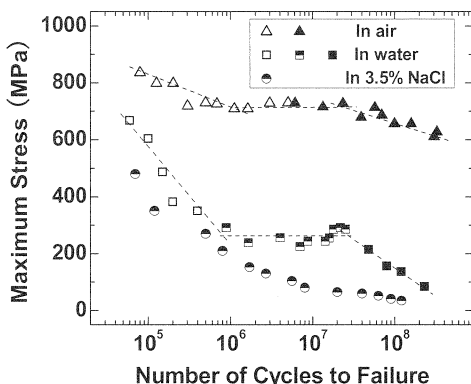


Fig. 2 S-N curves for specimens tested in air, water and 3.5%NaCl solution, hollow symbols: surface crack origination, solid symbols: subsurface origination, and semi-solid symbols: mixed mode origination.

For fatigue testing in water, a similar stepwise S-N curve is also presented (square symbols in Fig. 2), but the maximum stress value of transition part in the S-N curve, i.e. fatigue strength, is dramatically decreased, which (260MPa) is only 36% of that in laboratory air testing (720MPa). In high cycle regime, the fatigue strength with respect to the failure cycles of 10^5 is 600MPa, which is about 70% of the value obtained in the laboratory air testing. When failure cycles extends to 5×10^5 , the corresponding fatigue strength is 350MPa for water medium testing, which is only one half of the value obtained in the laboratory air testing. In VHCF regime, the difference of fatigue strength between the two cases is even larger, which indicates that the environmental effect of water on the degradation of fatigue strength is remarkable.

For fatigue testing in 3.5% NaCl solution, the S-N curve (circular symbols in Fig. 2) exhibits a continuously descending shape. The fatigue strength is even lower than that tested in water from low

cycle to VHCF regime, implying that the effect of 3.5% NaCl solution on the degradation of fatigue strength for the high strength steel is more remarkable than the case of testing in water medium.

The fatigue strength in aqueous solutions is substantially lower than that in laboratory air and the reduction increases gradually with decreasing stress level. This is further summarized as

$$\left. \frac{\sigma_{\max}^w}{\sigma_{\max}^a} \right|_{10^7} = 0.34 \quad \left. \frac{\sigma_{\max}^w}{\sigma_{\max}^a} \right|_{10^8} = 0.21, \quad (1)$$

and

$$\left. \frac{\sigma_{\max}^s}{\sigma_{\max}^a} \right|_{10^7} = 0.10 \quad \left. \frac{\sigma_{\max}^s}{\sigma_{\max}^a} \right|_{10^8} = 0.058, \quad (2)$$

where σ_{\max}^w is the fatigue strength tested in fresh water, σ_{\max}^s is that in 3.5% NaCl aqueous solution, and σ_{\max}^a is that in laboratory air.

Fatigue Crack Initiation. Unlike the testing case in laboratory air, for which the crack origination was a single origin for either surface or subsurface crack initiation, multiple fatigue crack origins were observed for the fatigue tests in water and in 3.5% NaCl solution (Fig. 3).

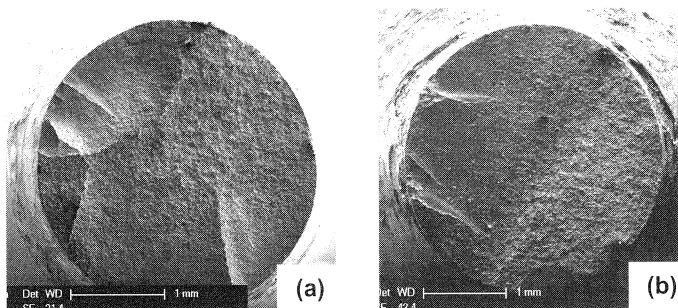


Fig.3 Fracture surfaces of multiple crack origins, (a) tested in water with $\sigma_{\max}^w = 286 \text{ MPa}$ and $N_f = 2.52 \times 10^7$, and (b) tested in 3.5% NaCl solution with $\sigma_{\max}^s = 41.3 \text{ MPa}$ and $N_f = 9.0 \times 10^7$.

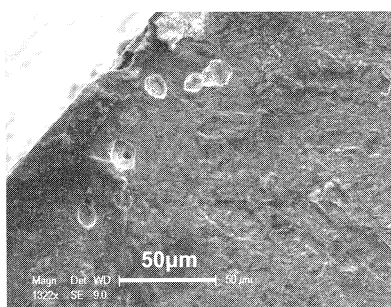


Fig.4 Fatigue crack initiation in water ($\sigma_{\max}^w = 286 \text{ MPa}$ and $N_f = 2.52 \times 10^7$), micro-void associated crack initiation.

The phenomenon of multiple crack origins for the cases tested in water and in 3.5% NaCl solution suggests that the probability of crack initiation under corrosive environment is greatly stimulated, which is attributed to the locally inhomogeneous stress concentration superimposed by the effect of aqueous medium, leading to the acceleration of fatigue damage process and to the degradation of the fatigue strength for the high strength steel tested. The phenomenon of multiple crack origins is one of the main features of fatigue crack initiation for high strength steel in aqueous environment.

Fig. 4 is an SEM micrograph showing fatigue crack initiation morphology of the specimen tested in water with $\sigma_{\max}^w = 286 \text{ MPa}$ and $N_f = 2.52 \times 10^7$. It is seen that

fatigue crack initiation in VHCF regime is surface crack initiation associated with subsurface micro-voids. This implies that crack damage may occur both at specimen surface and at subsurface inhomogeneities such as inclusions during fatigue crack initiation period. Then the surface cracking may coalesce with the growing micro-voids, leading to the early crack propagation. The formation of micro-voids at inhomogeneities is probably related to the joint effect of the mechanical loading

superimposed by aqueous environment. The phenomenon of micro-void related crack initiation was commonly observed in the specimens tested in water and in 3.5% NaCl solution. Most micro-voids involved in crack initiation were resulted from the decohesion of non-metallic inclusions.

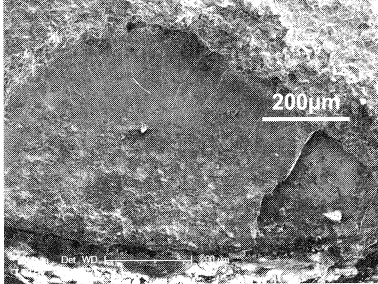


Fig. 5 Fractography (testing in 3.5% NaCl solution) with $\sigma_{\max}^s=130\text{MPa}$ and $N_f=2.68 \times 10^6$, showing crack initiation and early growth zone.

Fig. 5 shows fatigue crack initiation and early growth for the specimen tested in 3.5% NaCl solution, indicating surface damage associated with subsurface crack origin from an inclusion. This is early cracking stage of corrosion fatigue, i.e. cracks initiate at multiple sites of specimen surface layer by the process of surface damage combined with subsurface crack initiation, which is the result of mechanical cycling superimposed by the corrosive effect of test environment.

Fatigue Crack Propagation. For fatigue testing in air, fracture surface of early propagation zone is relatively smooth with transgranular cleavage-like morphology and fatigue striations. And for the crack steady propagation region, the fractography is quasi-cleavage morphology.

For the specimens tested in water and in 3.5% NaCl solution, the fracture surface morphology for fatigue crack steady growth is predominantly intergranular as shown in Fig. 6. From the measurements on SEM micrographs, the ratio of intergranular morphology is 75 % for the specimens tested in water, indicating that in water medium, fatigue crack growth along grain boundaries is a major mechanism. For the specimens tested in 3.5% NaCl solution, the ratio of intergranular morphology is 90%, indicating that crack growth along grain boundaries is a dominant mechanism.

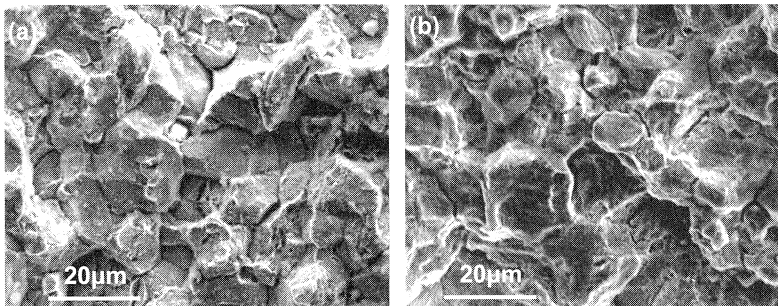


Fig. 6 Intergranular morphology of crack growth zone, (a) tested in water with $\sigma_{\max}^w=156\text{MPa}$ and $N_f=8 \times 10^7$, and (b) tested in 3.5% NaCl solution with $\sigma_{\max}^s=153\text{MPa}$ and $N_f=1.7 \times 10^6$.

From Fig. 6 (a) and (b), it is also seen secondary cracks along grain boundaries, which is the phenomenon of grain boundary embrittlement due to aqueous environmental effect. The presence of widespread secondary cracks was observed in the fatigue crack propagation period for the cases tested in water and in 3.5% NaCl solution.

For further observation of fatigue crack propagation, a group of V-notch specimens (7 pieces) was performed in 3.5% NaCl solution at $\sigma_{\max}^s=22.3\text{MPa}$. The observation on the fatigue terminated specimens tested in 3.5% NaCl solution showed that the typical morphology of multiple crack origins prevailed at specimen surface or subsurface covering almost the circumference of the notch root, and that a large portion of fracture surface resulted from corrosion fatigue cracking. The cracking area fraction of failed specimen is 65.2% obtained from image analysis.

The observations on fatigue terminated specimens showed fatigue crack initiation and early growth at surface and subsurface in the circumference of V-notch specimens. The fraction of fatigue cracking surface was small for the specimen terminated after 10^5 loading cycles and it increased with fatigue loading cycles until failure. The cracking area fraction of each specimen was identified and measured by image analysis with the results illustrated in Fig. 7, showing the obvious increase of cracking area fraction with the number of loading cycles.

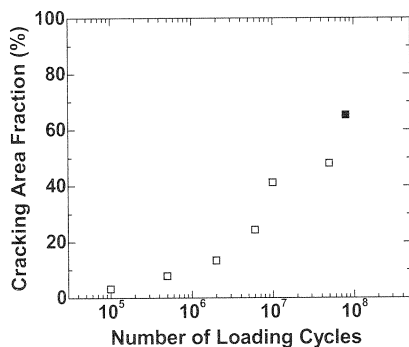


Fig. 7 Cracking area fraction vs. loading cycles for V-notch specimens, a solid symbol representing fatigue failure and hollow symbols representing terminated specimens prior to fatigue failure.

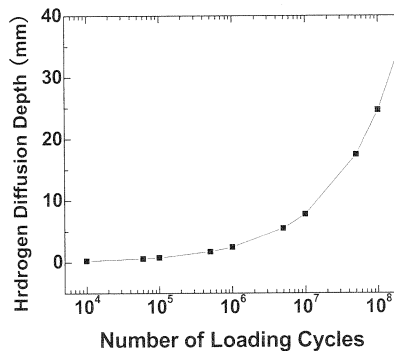


Fig. 8 Estimation of hydrogen diffusion depth vs. number of loading cycles.

Fatigue Mechanism. Under aqueous environment, the failure mechanism of high strength steel has been confirmed as hydrogen induced embrittlement [7,8]. One possible mechanism is assumed that the hydrogen is trapped by dislocations or at grain boundaries [7], and hydrogen effect is always superimposed by triaxial stress or stress concentration due to the heterogeneity of material to cause stress corrosion cracking or corrosion fatigue [8]. In the present investigation of fatigue behavior in the test environments of water and 3.5% NaCl solution for the structural steel, it was observed that multiple crack origins exist and the process of fatigue crack initiation and early growth is surface cracking associated with subsurface micro-voids, which is the typical evidence of hydrogen induced damage due to the effect of aqueous solution. It was also observed that the process of fatigue crack propagation is dominantly intergranular morphology, which is another typical evidence corresponding to hydrogen induced cracking in corrosion fatigue. In the process of hydrogen induced damage and failure, the diffusion and concentration of hydrogen is proportional to time variable t [9]:

$$X_d = 4\sqrt{D_H t} \quad (3)$$

where X_d is the maximum depth of hydrogen penetration due to lattice diffusion and D_H is the hydrogen diffusion coefficient of 10^{-5} mm²/s for similar structural steel [10]. Such that we may draw the variation tendency of X_d versus t , i.e. the number of loading cycles, as shown in Fig.8, by taking $t = N/f$ with f being the cycling frequency of 52.5Hz. It is noted that hydrogen induced corrosion fatigue is not only correlated to the diffusion depth but also to the concentration extent of hydrogen. Fig. 8 is just to show the increasing tendency of hydrogen penetration with time variable. Nevertheless, one may anticipate that a large time period for a specimen exposed to aqueous environment while cyclic loading will lead to larger value of hydrogen diffusion depth into the specimen and therefore more extensively corrosive effect of environment superimposed on the mechanical loading, which is the qualitative explanation for the cracking area increasing with loading cycles (Fig. 7) and for the large difference of fatigue strength between the cases tested in air and in aqueous solutions at higher failure lives, i.e. the fatigue strength is inversely proportional to fatigue failure cycles when introducing aqueous environment, as previously shown in Fig. 2.

Conclusions

The following conclusions are drawn from this investigation:

(1) In air environment, a stepwise shape S-N curve presents from high cycle to VHCF regimes. Fatigue crack initiation is of single origin and crack origination is subsurface mode at VHCF regime.

(2) In water and in 3.5% NaCl solution, fatigue strength is greatly degraded. The ratio of fatigue strength in water to that in air at the failure life of 10^7 is 34%, and the ratio reduces to 21% at 10^8 failure cycles. The ratio of fatigue strength in 3.5% NaCl solution to that in air is only 10% at 10^7 failure cycles, and is even lower of 5.8% at 10^8 failure cycles.

(3) The distinct characteristics of fractography for specimens tested in water and in 3.5% NaCl solution are (a) multiple crack origins, (b) surface cracking coalesced with subsurface growing micro-voids in crack initiation and early growth period, and (c) intergranular mode with widespread secondary cracks in crack steady propagation period. These are the evidences associated with hydrogen induced corrosion fatigue.

(4) For fatigue testing in 3.5% NaCl solution, the cracking area fraction of specimens increases with loading cycles which is also attributed to the effect of mechanical cycling superimposed by the corrosive action of environment.

Acknowledgments

This work was supported by the National Natural Science Foundation of China (Nos. 10772178 and 10721202) and the Knowledge Innovation Program of the Chinese Academy of Sciences (No. KJCX2-YW-L07).

References

- [1] S.E. Stanzl, E.K. Tschegg and H. Mayer: *Int. J. Fatigue* 8 (1986), p. 195
- [2] T. Naito, H. Ueda and M. Kikuchi: *Met. Trans. A* 15 (1984), p. 1431
- [3] N. Ranc, D. Wagner and P.C. Paris: *Acta Mater.* 56 (2008), p. 4012
- [4] G.M.D. Almaraz: *Mech. Mater.* 40 (2008), p. 636
- [5] T. Makino: *Int. J. Fatigue* 30 (2008), p. 1409
- [6] K. Tokaji, H-N. Ko, M. Nakajima and H. Itoga: *Mater. Sci. Eng. A* 345 (2003), p. 197
- [7] C.J. McMahon Jr: *Eng. Fract. Mech.* 68 (2001) p. 773
- [8] A. Nagao, S. Kuramoto, K. Ichitani and M. Kanno: *Scripta Mater.* 45 (2001), p. 1227
- [9] S.A. Shipilov: *Scripta Mater.* 47 (2002), p. 301
- [10] R.A. Page and W.W. Gerberich: *Met. Trans. A* 13 (1982), p. 305